Seasonal Dependence and Life Cycle of the Interannual Seesaw between the Aleutian and Icelandic Lows (Extended Abstract)

Tôhoku Geophys. Journ. (Sci. Rep. Tôhoku Univ., Ser. 5), Vol. 36, No. 2, pp. 171-176, 2001

Seasonal Dependence and Life Cycle of the Interannual Seesaw between the Aleutian and Icelandic Lows (Extended Abstract)

MEIJI HONDA[1], HISASHI NAKAMURA[1,2] and JINRO UKITA[3]

[1] IGCR, Frontier Research System for Global Change, 3173-25 Showa-machi, Kanazawa-ku, Yokohama, 236-0001
[2] Dept. Earth and Planetary Science, Univ. Tokyo, Tokyo 113-0033
[3] NASA, Goddard Space Flight Center, Greenbelt, Maryland 20771, U.S.A.

(Received December 11, 2000)

1. Introduction

The surface Aleutian and Icelandic lows (hereafter referred to as AL and IL) are wintertime semi-permanent low-pressure cells over the northern parts of the North Pacific (NP) and North Atlantic (NA), respectively (Fig. 1). Several previous studies pointed out that a seesaw-like oscillation exists between the AL and IL from one winter to another (*e.g.*, van Loon and Rogers 1978; Wallace and Gutzler 1981). In the present study (Honda *et al.* 2001), we shall investigate seasonal dependence and life cycle of the seesaw (AL-IL seesaw).

2. Data and analysis

Our analysis is based upon the 22-year (1973-1994) NMC (currently NCEP) operational analyses. Sea-level pressure (SLP), 250-hPa geopotential height (Z_{250}) and horizontal wind (U_{250} and V_{250}) were used. The daily AL and IL intensities were then defined as the respective minima in a 31-day moving-averaged SLP fields within given areas over the NP and NA as indicated in Fig. 1. The correlation coefficient between thus-defined AL and IL intensities was evaluated for each calendar day (Fig. 2). It becomes strongly negative only in February through mid-March. We henceforth refer to the 45-day period from January 31 to March 16 as the "peak period". The interannual variability in each of the AL and IL intensities for the "peak period" clearly indicates their seesaw-like relationship over the 22 winters (Fig. 3). To represent the strength and polarity of the seesaw, we defined the AL-IL index (AII) as the normalized IL-central pressure anomaly subtracted from the normalized AL-central pressure anomaly, both of which had been averaged over the "peak period" (Fig. 4).

To elucidate the spatial structure of the AL-IL seesaw, we show the SLP composite difference between five strongest positive and negative years for the "peak period". The seesaw is evident in this difference composite map (Fig. 5a). A corresponding seesaw is evident in the middle and upper troposphere for the "peak period" (Fig. 5b). In recognition of this equivalent barotropic structure as depicted in Fig. 5, we hereafter focus on the time evolution of the upper-tropospheric seesaw that appears in the Z_{250} field.

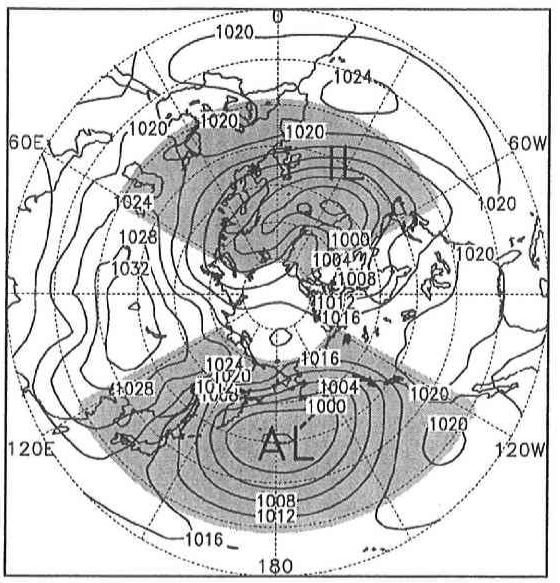

Fig. 1. Climatological-mean sea-level pressure (hPa) for January over the Northern Hemisphere. AL and IL denote the Aleutian and Icelandic lows, respectively. Two regions are shaded where the lowest pressures were identified, separately, for defining their intensities (after Honda *et al.* 2001).

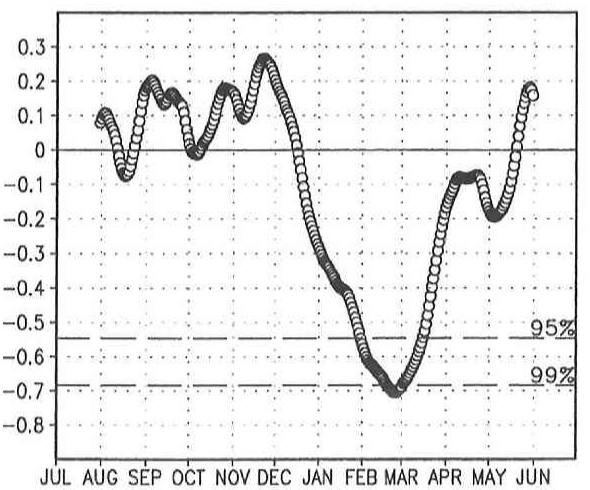

Fig. 2. Correlation coefficient between the 22-year timeseries of the 31-day moving-averaged AL and IL intensities for each calendar day. Dashed lines correspond to the 95% and 99% confidence levels, as indicated, with 11 degrees of freedom (half of 22 years) assumed (after Honda *et al.* 2001).

3. Life cycle of the AL-IL seesaw

Next, we investigated a typical seasonal evolution of the seesaw in the linear lag regression maps between the AII and mean Z_{250} anomalies for each of the nine 45-day periods, whose central calendar days are mutually 15 days apart, from early December to early April. We focus on a

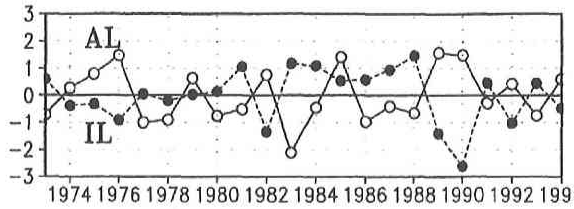

Fig. 3. Interannual variations (from 1973 to 1994) of the standardized AL (thin line with open circles) and IL (dashed line with solid circles) intensities averaged between January 31 and March 16 (i.e., in the "peak period") (after Honda *et al.* 2001).

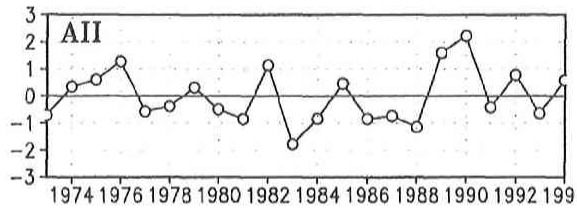

Fig. 4. Time series of the standardized Aleutian low-Iceland low index (AII) for the "peak period" for 1973-1994 (after Honda *et al.* 2001).

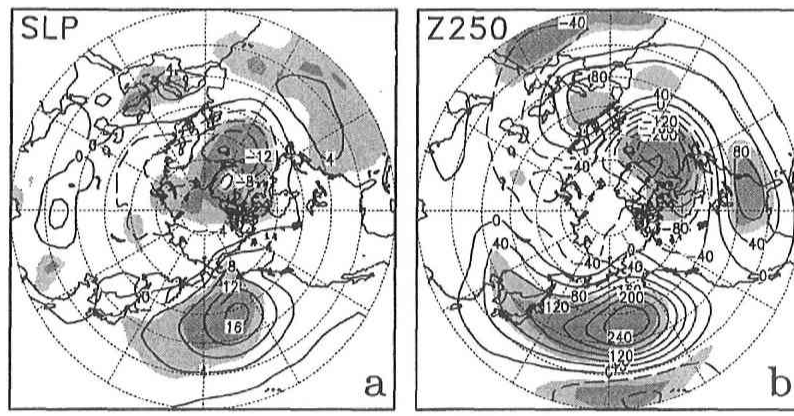

Fig. 5. Composite differences of (a) sea-level pressure (hPa) and (b) 250-hPa geopotential height (m) obtained by subtracting the composites for the five strongest negative AII years (stronger AL; 1981, 1983, 1984, 1986 and 1988) from those for the five strongest positive AII years (stronger IL; 1976, 1982, 1989, 1990 and 1992) based upon the 45-day mean for January 31-March 16 ("peak period"). Shaded lightly and heavily where the differences are significant with the 95% and 99% confidence levels, respectively (after Honda *et al.* 2001).

typical winter situation for the weaker AL with the stronger IL (*i.e.*, positive AII).

In December, upper-tropospheric anticyclonic anomalies corresponding to the weaker AL gradually develop over the eastern NP (Figs. 6a and 6b). Then, a Pacific/North American (PNA) pattern-like wavetrain emanates from the anticyclonic anomalies in early January (Fig. 6c). During the same period, another wavetrain emanates from the end of the PNA-like wavetrains.

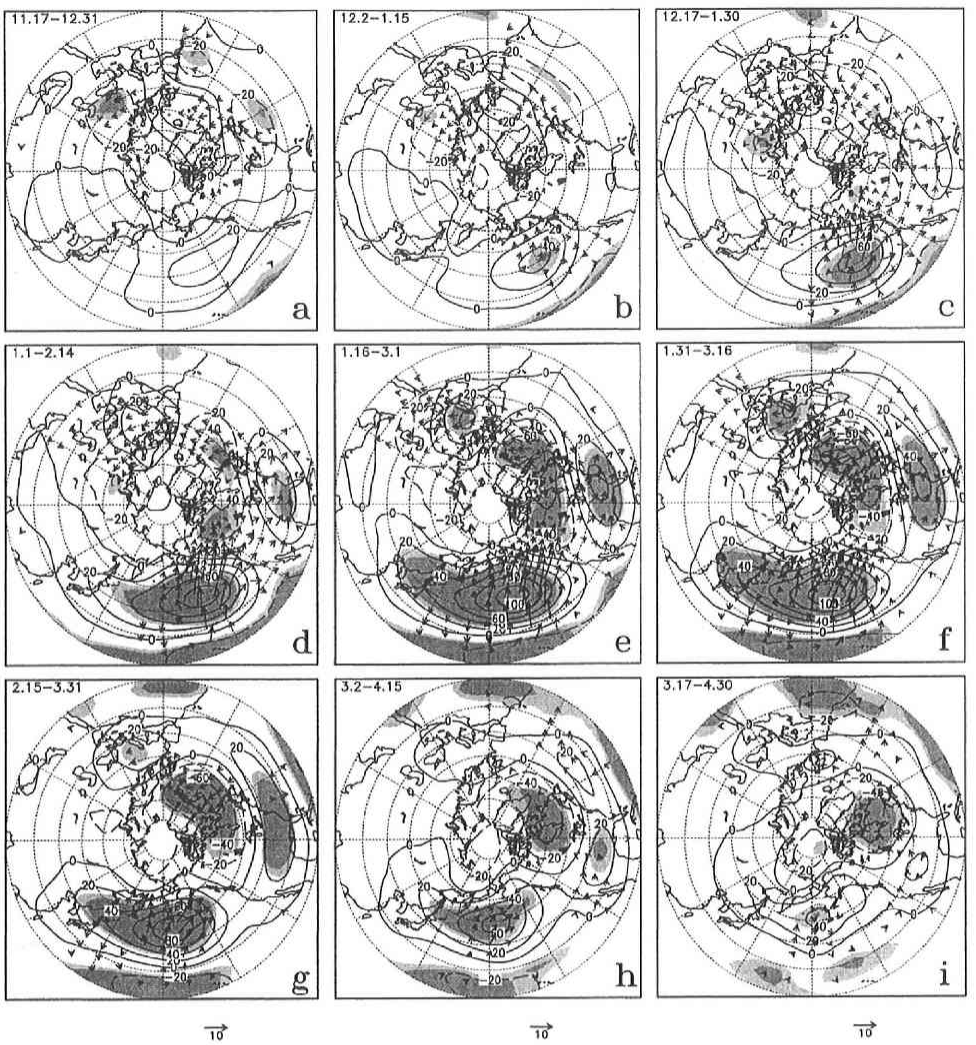

Fig. 6. Maps of the linear lag regression coefficient between the AL-IL index (AII) and 250-hPa geopotential height (Z_{250}) averaged for each of nine 45-day periods, which loosely correspond to early December, late December, early January, ..., and early April (November 17-December 31, December 2-January 15, ..., and March 17-April 30). The coefficient corresponds to a local change in height (m) when the AII increases by its unit standard deviation. Areas of light and heavy shading indicate the AII-Z_{250} correlation is significant with the 90% and 95% confidence levels, respectively, based upon the t-statistic with 11 degrees of freedom (half of 22 years) assumed. Arrows indicate the horizontal component of the wave activity flux ($m^2\ s^{-2}$; scaled as at the bottom) formulated by Takaya and Nakamura (1997) (after Honda *et al.* 2001).

Thus, negative anomalies, corresponding to stronger IL, appear over the NA. These two wavetrains become most prominent in late January (Fig. 6d). A diagnosis based upon the wave-activity flux formulated by Takaya and Nakamura (1997) suggests that these anomalies are associated with stationary Rossby wavetrains. Although the wavetrain across North America gradually weakens during February (Figs. 6e and 6f), both anomalies over the two oceans further

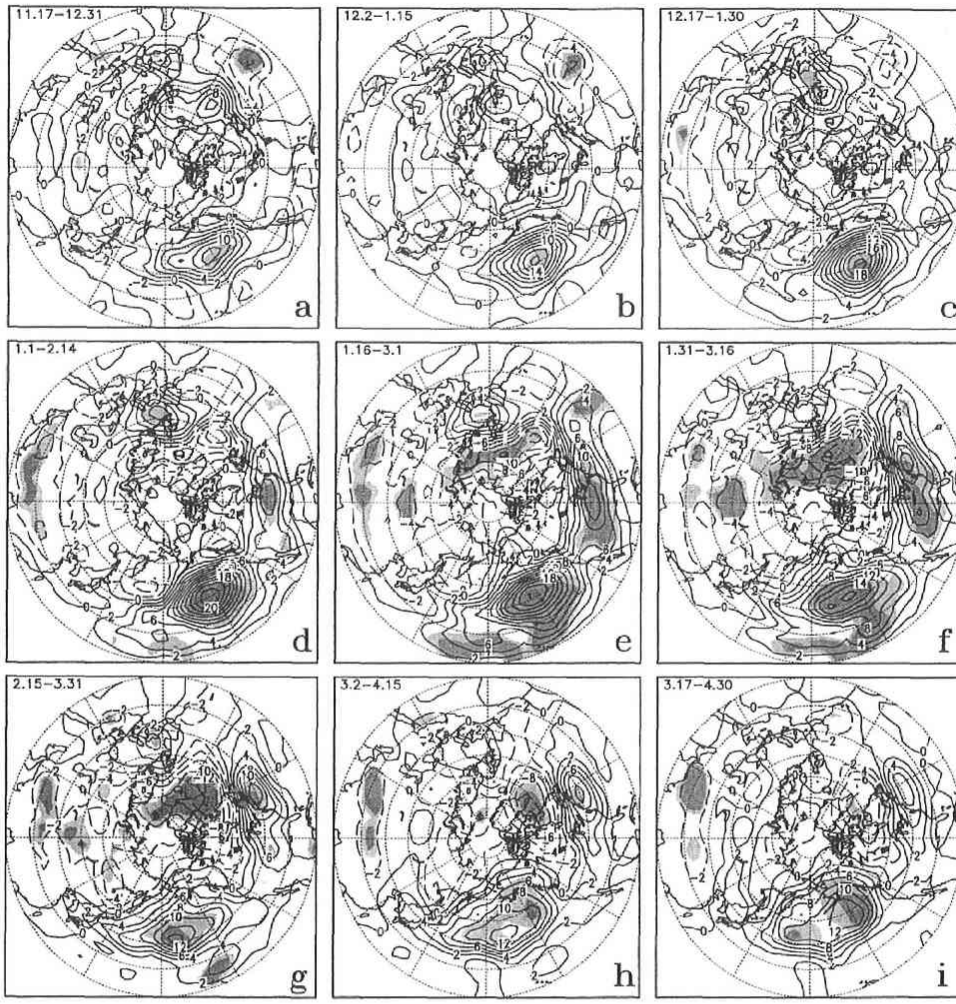

Fig. 7. As in Fig. 6, but for the linear lag regression coefficients between the AII and the tendency in 250-hPa geopotential height (m day^{-1}) induced solely by the anomalous vorticity flux convergence associated with migratory eddies along stormtracks. The flux was evaluated from 8-day high-pass filtered wind field at the 250-hPa level, as in Nakamura *et al.* (1997) (after Honda *et al.* 2001).

develop. Through the above sequence, the AL–IL seesaw becomes fully developed in the "peak period" (Fig. 6f). The anticyclonic anomalies over the NP start decaying right after this period while the IL anomalies remain strong until early April (Figs. 6g–6i).

The feedback forcing from transient eddies migrating along anomalous stormtracks is likely to contribute towards the development and maintenance of stationary anomalies (*e.g.*, Lau and Nath 1991). In order to investigate a seasonal evolution of the barotropic feedback forcing from the transient eddies at the 250-hPa level, we computed the linear lag regression coefficient between the AII and the anomalous feedback forcing for each of the nine 45-day periods. In the NP, significant anticyclonic feedback forcing through the anomalous vorticity flux divergence upon the anticyclonic stationary anomalies throughout winter (Fig. 7). In contrast, no significant

eddy feedback forcing is observed over the NA until January (Figs. 7a-7d). It is after the development of the cyclonic anomalies in January that the significant cyclonic feedback forcing from more active eddies through the anomalous vorticity flux convergence contributes to the anomalous deepening of the surface IL and NAO-like anomalies aloft (Figs. 6, 7e and 7f). This feedback continues throughout the "peak period" and even until late March, acting to maintain the cyclonic anomalies over the NA (Figs. 7g-7i).

4. Conclusions

It became apparent through our analysis that the interannual seesaw-like oscillation between the AL and IL intensities distinctly appears only in late winter (February to mid-March; Fig. 2) and that the AL and IL anomalies which constitute the seesaw do not start developing simultaneously over the NP and NA in the course of a particular winter season (Fig. 6). Rather, the seesaw formation is triggered by the propagation of wave activity accumulated over the NP in early- through mid-winter towards the NA in the form of a PNA-like Rossby wavetrain across North America. The IL anomalies appear to be initiated as a component of another wavetrain across the NA emanating from the southeastern U.S. at the leading edge of the PNA-like wavetrain (Figs. 6c and 6d). The IL anomalies thus formed amplify through the feedback forcing from the enhanced (suppressed) stormtrack activities in the presence of the intensified (weakened) westerlies along the NA jet throughout late winter (Fig. 7). In this manner, the feedback contributes to the seesaw development also over the NA, in spite of the weakening of the Rossby wavetrain across North America after January. This study suggests that the atmospheric variability in late winter over the NA is significantly influenced by the variability in early- and mid-winter over the NP. Influence of the AL-IL seesaw on the leading variability in the NH (Arctic Oscillation: Thompson and Wallace 1998) is briefly discussed in Nakamura and Honda (2001) in this issue and details in Honda and Nakamura (2001).

References

Honda, M., H. Nakamura, J. Ukita, I. Kousaka and K. Takeuchi, 2001: Interannual seesaw between the Aleutian and Icelandic lows. Part I: Seasonal dependence and life cycle, *J. Climate*, **14**, 1029-1042.

Honda, M. and H. Nakamura, 2001: Interannual seesaw between the Aleutian and Icelandic lows. Part II: Its significance in the Interannual variability over the wintertime Northern Hemisphere, *J. Climate*, in press.

Lau, N.-C. and M.J. Nath, 1991: Variability of the baroclinic and barotropic transient eddy forcing associated with monthly changes in the midlatitude storm tracks, *J. Atmos. Sci.*, **48**, 2589-2613.

Nakamura, H. and M. Honda, 2001: Aleutian-Icelandic low seesaw and its relationship with the Arctic Oscillation, *this issue*.

Nakamura, H., M. Nakamura and J.L. Anderson, 1997: The role of high- and low-frequency dynamics in blocking formation, *Mon. Wea. Rev.*, **125**, 2074-2093.

Takaya, K. and H. Nakamura, 1997: A formulation of a wave-activity flux for stationary Rossby waves on a zonally varying basic flow, *Geophys. Res. Lett.*, **24**, 2985-2988.

Thompson, D.W.J. and J.M. Wallace, 1998: The Arctic Oscillation signature in the wintertime geopotential height and temperature fields, *Geophys. Res. Lett.*, **25**, 1297-1300.

van Loon, H. and J.C. Rogers, 1978: The seesaw in winter temperatures between Greenland and Northern Europe. Part I: General description, *Mon. Wea. Rev.*, **106**, 296-310.

Wallace, J.M. and D.S. Gutzler, 1981: Teleconnections in the geopotential height field during the Northern Hemisphere winter, *Mon. Wea. Rev.*, **109**, 784-812.